Hydrocarbon-Bridged Complexes. 15.[1] Molecular and Electronic Structures of (μ-Ethynediyl)bis(pentacarbonylrhenium), $(OC)_5ReC{\equiv}CRe(CO)_5$

Jürgen Heidrich, Manfred Steimann, Mathilde Appel, and Wolfgang Beck*

Institut für Anorganische Chemie der Universität München, D-8000 München 2, FRG

Julia R. Phillips and William C. Trogler*

Department of Chemistry, University of California, San Diego, D-006, La Jolla, California 92093-0506

Received November 28, 1989

The structure of $(OC)_5ReC{\equiv}CRe(CO)_5$ has been determined by single-crystal X-ray analysis. Crystal data: space group $P\bar{1}$, $Z = 1$, $a = 652.8$ (2), $b = 651.6$ (2), $c = 987.2$ (2) pm, $\alpha = 90.40$ (2), $\beta = 96.77$ (3), $\gamma = 98.62$ (3)°. The two $Re(CO)_5$ groups are arranged in the eclipsed conformation. The C≡C bond length (119 (3) pm) parallels that in ethyne. The Re–C bond (214 (2) pm) is significantly shorter than that in $(OC)_5ReCH_2CH_2Re(CO)_5$ (230 (1) pm). The UV-visible spectrum of $(OC)_5ReC{\equiv}CRe(CO)_5$ in THF shows absorptions at 319 (12000 M^{-1} cm^{-1}), 242 (50000 M^{-1} cm^{-1}), and 223 nm (68000 M^{-1} cm^{-1}). Cyclic voltammetry measurements in acetonitrile reveal two irreversible oxidations at +1.02 and +1.55 V vs an Ag wire reference. SCF-Xα-DV calculations for D_{4h} $(OC)_5ReC{\equiv}CRe(CO)_5$ show that the highest occupied molecular orbital, $13e_u$, derives from the C≡C π bond. Little mixing between the C≡C π, π^*, or σ orbitals occurs, so that the bonding is similar to ethyne. The predominant bonding between Re and the acetylide carbons involves mixing of p_z–d_{z^2} hybrid orbitals on rhenium with the a_{1g} and a_{2u} combinations of the acetylide lone pairs. Although the C≡C triple bond is relatively unperturbed, a high negative charge density predicted for this fragment results in a lower oxidation potential for $(OC)_5ReC{\equiv}CRe(CO)_5$ as compared to $Re_2(CO)_{10}$. Also, the lowest energy-allowed electronic transition at 319 nm is assigned to the $13e_u$ (C≡C π) → $13e_g$ (CO π^*) one-electron excitation ($^1A_{1g} \rightarrow {}^1A_{2u}$).

Recently the Munich group[2] reported the synthesis of the σ,σ-acetylide-bridged complex $(OC)_5ReC{\equiv}CRe(CO)_5$ (1). The organometallic Lewis acid[3] $(OC)_5ReFBF_3$ reacts with $HC{\equiv}CSiMe_3$ to form the σ,π-ethynide bridged complex $[(OC)_5Re(\mu\text{-}\eta^1{:}\eta^2\text{-}C{\equiv}CH)Re(CO)_5]^+BF_4^-$, which upon deprotonation gives 1 in good yields. Complex 1 is not formed by metathesis of Na_2C_2 (or Li_2C_2) with $Re(CO)_5FBF_3$.[4] Similarly the reaction of Na_2C_2 or Li_2C_2 with $Mn(CO)_5Br$ gives $Mn_2(CO)_{10}$ instead of $(OC)_5MnC{\equiv}CMn(CO)_5$.[5] Examples of σ,σ-ethynide-bridged metal complexes[6] include those of gold(I),[7] palladium(II), platinum(II),[8a] and tungsten[8b] as well as those for a number of main-group metals.[9] Other interesting complexes that contain a C_2-bridging unit are $(t\text{-}BuO)_3W{\equiv}C{-}C{\equiv}W(O\text{-}t\text{-}Bu)_3$,[10a] $(t\text{-}Bu_3SiO)_3Ta(\mu\text{-}C_2)Ta(OSi\text{-}t\text{-}Bu_3)_3$,[10b] and $(R_3P)_2Pt[C_2W_2(O\text{-}t\text{-}Bu)_5]_2$.[10c]

Table I. Atomic Coordinates (×10⁴) and Isotropic Thermal Parameters ($pm^2 \times 10^{-1}$)

	x	y	z	U
Re(1)	3128 (1)	1308 (1)	2598 (1)	43 (1)
C(1)	2504 (29)	3685 (25)	3708 (19)	62 (5)
O(1)	2182 (33)	4983 (25)	4378 (19)	93 (7)
C(2)	709 (44)	-457 (26)	3067 (16)	76 (8)
O(2)	-884 (27)	-1433 (25)	3350 (21)	98 (7)
C(3)	3911 (31)	-1160 (26)	1715 (19)	62 (5)
O(3)	4343 (32)	-2580 (26)	1200 (19)	97 (7)
C(4)	5780 (54)	3013 (30)	2360 (17)	84 (10)
O(4)	7549 (28)	3714 (26)	2255 (20)	94 (7)
C(5)	1751 (29)	2264 (25)	900 (16)	59 (5)
O(5)	892 (29)	2779 (26)	-108 (14)	89 (6)
C(6)	4593 (27)	277 (24)	4473 (17)	53 (4)

Table II. Bond Lengths (pm) and Bond Angles (deg) for 1

Re(1)-C(1)	201.0 (18)	Re(1)-C(2)	191.5 (24)
Re(1)-C(3)	198.4 (19)	Re(1)-C(4)	195.2 (30)
Re(1)-C(5)	195.8 (16)	Re(1)-C(6)	214.1 (16)
C(1)-O(1)	112.9 (26)	C(2)-O(2)	119.9 (30)
C(3)-O(3)	113.9 (27)	C(4)-O(4)	119.3 (38)
C(5)-O(5)	116.0 (22)	C(6)-C(6a)	119.5 (33)
C(1)-Re(1)-C(2)	91.5 (8)	C(1)-Re(1)-C(3)	172.9 (7)
C(2)-Re(1)-C(3)	87.7 (8)	C(1)-Re(1)-C(4)	87.3 (9)
C(2)-Re(1)-C(4)	172.2 (8)	C(3)-Re(1)-C(4)	92.5 (9)
C(1)-Re(1)-C(5)	93.1 (7)	C(2)-Re(1)-C(5)	95.5 (8)
C(3)-Re(1)-C(5)	94.0 (7)	C(4)-Re(1)-C(5)	92.3 (8)
C(1)-Re(1)-C(6)	86.2 (7)	C(2)-Re(1)-C(6)	83.9 (7)
C(3)-Re(1)-C(6)	86.8 (7)	C(4)-Re(1)-C(6)	88.3 (8)
C(5)-Re(1)-C(6)	179.0 (7)	Re(1)-C(1)-O(1)	177.2 (17)
Re(1)-C(2)-O(2)	175.0 (19)	Re(1)-C(3)-O(3)	179.4 (13)
Re(1)-C(4)-O(4)	167.6 (21)	Re(1)-C(5)-O(5)	178.0 (12)
Re(1)-C(6)-C(6a)	179.2 (23)		

Results and Discussion

Structure of $(OC)_5ReC{\equiv}CRe(CO)_5$ (1). Crystals of 1 to be used for X-ray crystallographic analysis have been obtained from THF solution. Atom positions and bond

(1) Hydrocarbon-bridged complexes, part 15. Part 14: Beck, W.; Niemer, B. *Angew. Chem.* **1989**, *101*, 1699; *Angew. Chem., Int. Ed. Engl.* **1989**, *28*, 1705.
(2) Appel, M.; Heidrich. J.; Beck, W. *Chem. Ber.* **1987**, *120*, 1087.
(3) Beck, W.; Sünkel, K. *Chem. Rev.* **1988**, *88*, 1405.
(4) Raab, K. Dissertation, University of Munich, 1984.
(5) Manning, M. C.; Trogler, W. C. *Inorg. Chim. Acta* **1981**, *50*, 247.
(6) Reviews: Nast, R. *Coord. Chem. Rev.* **1982**, *47*, 89. Holton, J.; Lappert, M. F.; Pearce, R.; Yarrow, P. I. W. *Chem. Rev.* **1983**, *83*, 135.
(7) Nast, R.; Kirner, U. *Z. Anorg. Allg. Chem.* **1964**, *330*, 311. Nast, R.; Schneller, P.; Hengefeld, A. *J. Organomet. Chem.* **1981**, *214*, 273. Cross, R. J.; Davidson, M. F. *J. Chem. Soc., Dalton Trans.* **1986**, *411*.
(8) (a) Ogawa, H.; Onitsuka, K.; Takashi, J.; Takahashi, S.; Yamamoto, Y.; Yamazaki, H. *Organometallics* **1988**, *7*, 2257, and references therein. (b) Ustynyuk, N. A.; Vinogradova, V. N.; Kravtsov, D. N. *Organomet. Chem. USSR* **1988**, *1*, 45.
(9) Davidsohn, W. E.; Henry, M. C. *Chem. Rev.* **1967**, *67*, 73, and references therein.
(10) (a) Listemann, M. L.; Schrock, R. R. *Organometallics* **1985**, *4*, 74. (b) LaPointe, R. E.; Wolczanski, P. T.; Mitchell, J. F. *J. Am. Chem. Soc.* **1986**, *108*, 6382. Neithamer, D. R.; LaPointe, R. E.; Wheeler, R. A.; Richeson, D. S.; Van Duyne, G. D.; Wolczanski, P. T. *J. Am. Chem. Soc.* **1989**, *111*, 9056. (c) Blau, R. J.; Chisholm, M. H.; Folting, K.; Wang, R. J. *J. Am. Chem. Soc.* **1987**, *109*, 4552.

0276-7333/90/2309-1296$02.50/0

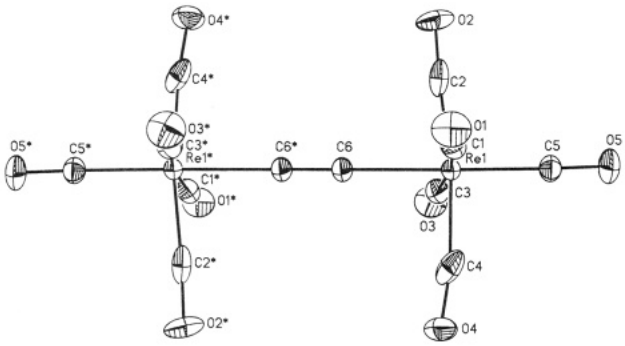

Figure 1. Molecular structure of $(OC)_5ReC{\equiv}CRe(CO)_5$ (**1**) in the crystal (at 20% probability level).

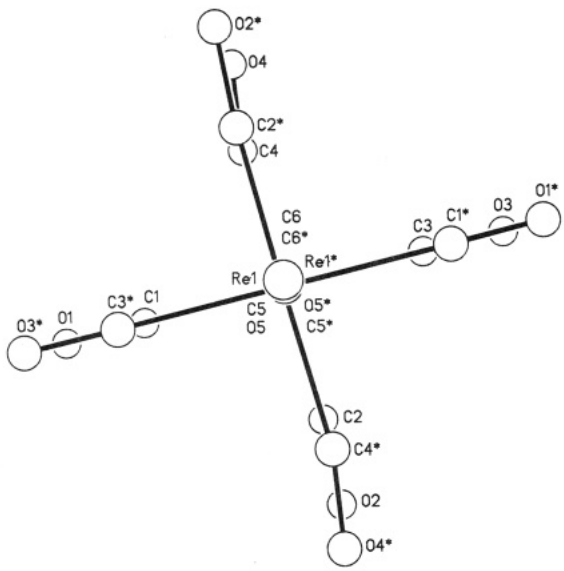

Figure 2. Another view on the molecular structure of **1**.

Table III. C–C and M–C Bond Lengths (pm) in 1–4

	C–C	M–C
1	119 (3)	214 (2)
2[13]	132.0 (5)	214.8 (3), 216.0 (3)
3a[14]	137 (1)	217, 218 (1)
3b[15]	138 (3)	222 (2), 221 (2)
4[12]	152.2 (17)	230.4 (8)

length and bond angle parameters are presented in Tables I and II. The molecule is oriented around a crystallographic center of symmetry. As shown in Figure 1 the rhenium atom, the acetylide carbon atom, and the axial carbonyl group are collinear. The two $Re(CO)_5$ groups are arranged in an ideal eclipsed conformation (Figure 2), in contrast to the staggered conformation of solid $Re_2(CO)_{10}$[11] and of $I(Me_3P)_2PtC{\equiv}CPt(PMe_3)_2I$.[8a] As in $Re_2(CO)_{10}$ and $(OC)_5ReCH_2CH_2Re(CO)_5$,[12] the equatorial carbonyl groups are bent away from the axial carbonyl ligand. The distance between the rhenium atom and the plane defined by the O1, O2, O3, and O4 atoms is 24 pm. The carbon–carbon distance of **1** is similar to that in $I(Me_3P)_2PdC{\equiv}CPd(PMe_3)_2I$ (118 (5) pm),[8a] whereas for $(t\text{-}Bu_3SiO)_3TaC_2Ta(OSi\text{-}t\text{-}Bu_3)_3$[10b] the bonding is best described as a cumulene Ta=C=C=Ta (C–C 137 (4) pm). Of interest is a comparison of bond lengths in **1–4** (Scheme I and Table III).

Table IV. Composition of Upper Valence Orbitals of 1

orbital	energy, eV	Re	C_2	CO_{ax}	CO_{eq}
11 e_u	−10.86			95%	CO 1p
3 b_{2g}	−8.29	72% d_{xy}			28% π*
3 b_{1u}	−8.29	72% d_{xy}			28% π*
16 a_{2u}	−8.24	12% p_z–d_{z^2}	78% sp_z lp	5%	5%
12 e_u	−8.17	72% $d_{xz,yz}$	5% π	9% π*	14% π*
12 e_g	−8.04	75% $d_{xz,yz}$		10% π*	15% π*
17 a_{1g}	−7.05	26% p_z–d_{z^2}	56% sp_z lp	7%	7%
13 e_u[a]	−5.39	8% $d_{xz,yz}$	80% π	7%	4%
13 e_g	−3.43	4% $d_{xz,yz}$		29% π*	66% π*
17 a_{2u}	−3.36	1%	9%	5% π*	85% π*
14 e_u	−3.33	3%	2%	8% π*	87% π*
18 a_{1g}	−3.25	5%	11%	7% π*	77% π*
14 e_g	−3.08	6% $d_{xz,yz}$		45% π*	50% π*

[a] Highest occupied orbital.

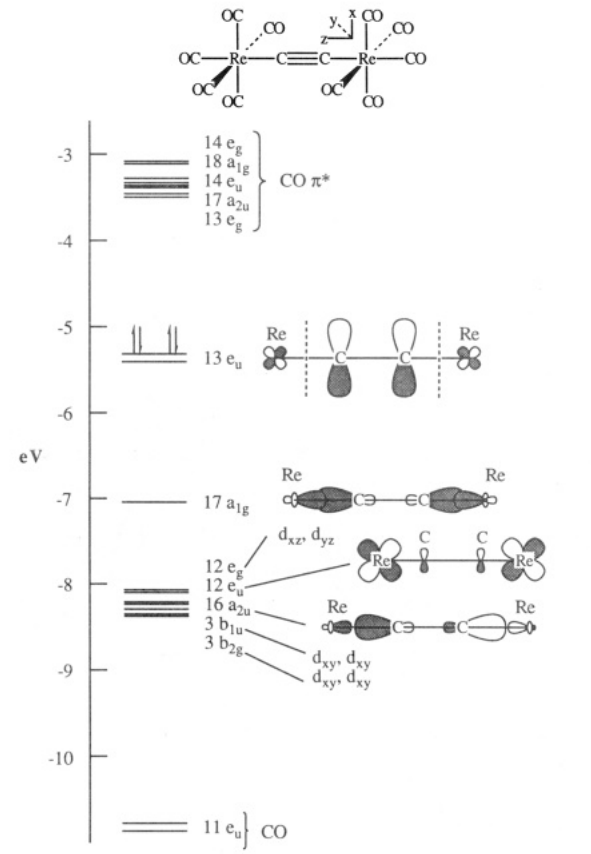

Figure 3. Molecular orbital diagram obtained from SCF-Xα-DV calculations of **1**.

The C–C bonds between the two metal atoms in **1**, **2**, and **4** are practically identical with that in ethyne (120 pm), ethene (134 pm), and ethane (153 pm), respectively. The shortening of the rhenium carbon distance from **4** to **1** reflects the increasing s character of carbon as observed for organic derivatives. The compounds **3a,b** do not fit perfectly into this series, due to the neighboring keto groups. Both the C≡C and Re–C lengths of **1** indicate that there is very small, if any, interaction between C≡C p_π and Re d_π orbitals. This finding is in agreement with the spectroscopic data:[2] The ^{13}C chemical shift of **1** (94 ppm) is very near to that of organic acetylenes and the CO stretching frequencies of **1** (2135, 2032, 1974 cm^{-1}, CH_2Cl_2) are not very different from that of $(OC)_5ReCH_2CH_2Re(C$-

(11) Dahl, L. F.; Ishishi, E.; Rundle, R. E. *J. Chem. Phys.* **1957**, *26*, 1750. Churchill, M. R.; Amoh, K. N.; Wasserman, H. J. *Inorg. Chem.* **1981**, *20*, 1609.
(12) Raab, K.; Nagel, U.; Beck, W. *Z. Naturforsch. Teil B* **1983**, *38*, 1466.
(13) Breimair, J.; Steimann, M.; Wagner, B.; Beck, W. *Chem. Ber.* **1990**, *123*, 7.
(14) Beck, W.; Schweiger, M.; Müller, G. *Chem. Ber.* **1987**, *120*, 889.
(15) Schweiger, M. Dissertation, University of Munich, 1988.

Scheme I

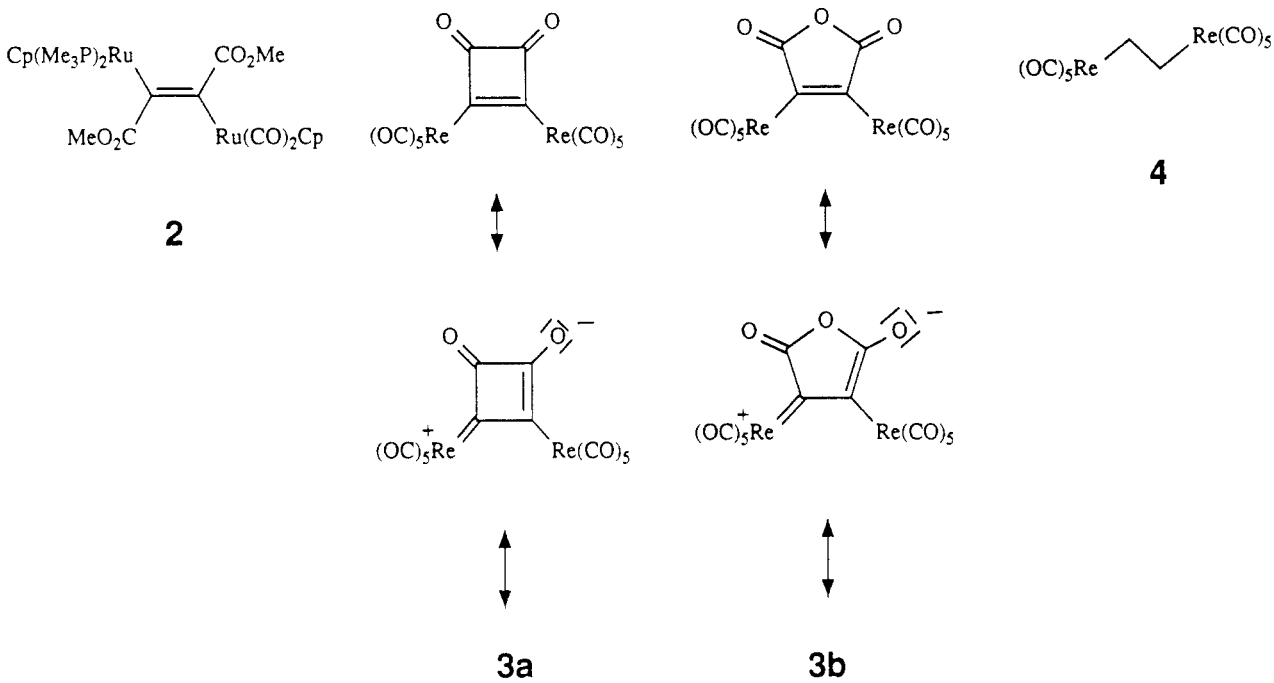

$O)_5$ (2111, 2012, 1980 cm^{-1}, cyclohexane) and of $H_3CRe(CO)_5$ (2132, 2005, 1950 cm^{-1}, CH_2Cl_2).

Electronic Structure of 1. Results of SCF-Xα-DV calculations of **1** are summarized in Table IV and in Figure 3. Of particular interest are the interactions that occur between the two rhenium atoms and the bridging acetylide ligand. The atomic charges calculated for Re (+0.86), the acetylide fragment (−0.56), and carbonyl group (−0.12) suggest a high charge density on the bridging C_2 unit. This results in a 13 e_u HOMO, which predominantly consists of the doubly degenerate C≡C π-bonding orbital. Only a small mixing (5–8%) between the acetylide π orbitals and the Re(d_{xz},d_{yz}) orbitals occurs in the 13 e_u and 12 e_u orbitals, which correspond to Re–C π-antibonding and π-bonding orbitals, respectively. Because both orbitals are occupied, there is no net rhenium–acetylide π interaction. The σ component of the C≡C triple bond is localized (97%) in a deep-lying 11 a_{1g} orbital at −17.67 eV. Thus the acetylide triple bond is relatively unperturbed in the complex. The dominant interaction between the rhenium and acetylide can be regarded as a σ-bond from the a_{1g} and a_{2u} combinations of the two acetylide lone pairs with p_z–d_{z^2} hybrid orbitals of appropriate symmetry on the metal. This interaction appears in the 16 a_{2u} and 17 a_{1g} orbitals of Figure 3. Other occupied d orbitals (3 b_{2g}, 3 b_{1u}, 12 e_g) participate in rhenium–carbon monoxide backbonding, which is typical of metal carbonyl complexes. Essentially no Re → acetylide π backbonding occurs because the acetylide 16 $e_g\pi^*$ orbital is calculated to lie high above valence orbitals at +3.16 eV. The overall picture of an intact C≡C triple bond and two Re–C σ bonds agrees with the structural results described earlier and differs from that observed in $(t\text{-}Bu_3SiO)_3Ta(\mu\text{-}C_2)Ta(OSi\text{-}t\text{-}Bu_3)_3$. In the latter complex the long C≡C bond of 1.32 (4) Å and the results of EH calculations suggest appreciable dπ → C_2 (π^*) backbonding. The difference in the two cases may be attributed to the opposite roles played by π-acceptor CO ligands in **1** and π-donor siloxide ligands in the tantalum dimer in determining the energy of the dπ orbitals relative to the C_2 fragment.

One interesting aspect of the calculations is the prediction of the degenerate C≡C π orbitals as the HOMO.

Table V. Transition State Calculations for 1

Ionization Potentials

orbital	IP, eV	orbital	IP, eV
13 e_u	8.17	16 a_{2u}	10.25
17 a_{1g}	9.50	3 b_{1u}	10.37
12 e_g	10.11	3 b_{2g}	10.37
12 e_u	10.22	11 e_u	12.90

Transition Energies

one-electron transition	dipole allowed	ΔE, cm^{-1}
13 e_u → 17 a_{2u}	no	21 800
13 e_u → 13 e_g	yes	21 900
13 e_u → 14 e_g	yes	24 500
17 a_{1g} → 13 e_g	no	34 000
17 a_{1g} → 17 a_{2u}	yes	34 200
17 a_{1g} → 14 e_u	yes	34 200
12 e_g → 13 e_g	no	38 400
12 e_g → 17 a_{2u}	yes	38 400

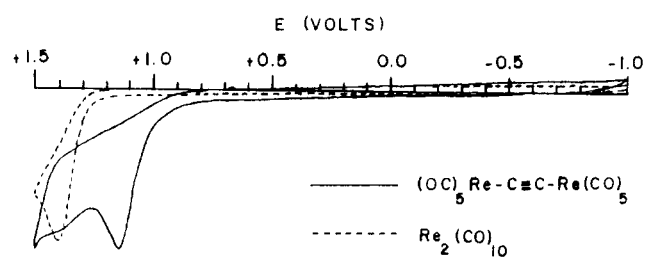

Figure 4. Cyclic voltammograms of **1** and $Re_2(CO)_{10}$ in CH_2Cl_2. The supporting electrolyte was 0.1 M tetra-*n*-butylammonium perchlorate, and the scan rate was 100 mV/s.

Transition state calculations (Table V) suggest that the first ionization (in the gas phase) should also arise from this orbital. In this context we note that **1** undergoes an irreversible oxidation process with E_{p_a} 1.12 V (100 mV/s scan) vs Ag wire in dichloromethane solvent (Figure 4). A second poorly resolved oxidation occurs near 1.35 V. Similar behavior is observed in acetonitrile solvent with peaks at 1.02 and 1.55 V in the cyclic voltammogram. No reduction processes were observed to −2.1 V in THF solvent. The oxidation behavior can be compared to $Re_2(CO)_{10}$, whose first irreversible oxidation wave occurs with

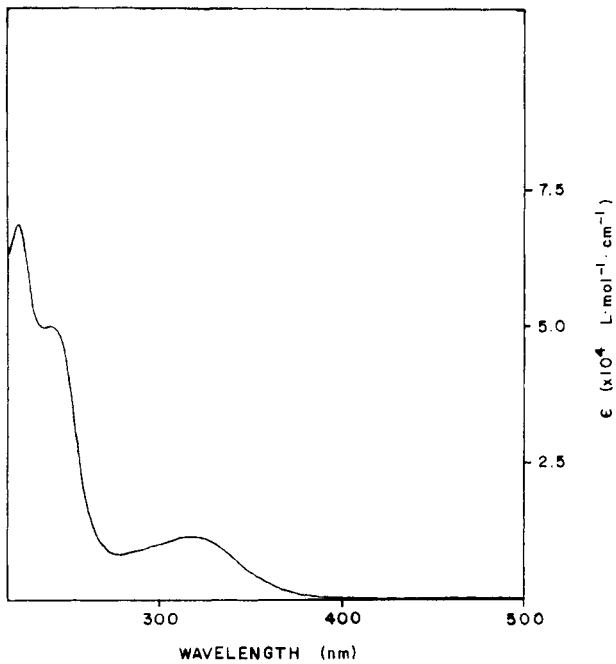

Figure 5. Electronic absorption spectrum of 9.3×10^{-6} M 1 in THF.

E_{p_a} = 1.40 V in acetonitrile or dichloromethane (Figure 4). Thus, the acetylenic moiety in 1 oxidizes more easily than the metal–metal bond in $Re_2(CO)_{10}$. This probably results from a high negative charge density on the σ,σ-ethynide fragment in 1, as suggested by the Xα calculations. Although the carbon–carbon triple bond in 1 is perturbed little by binding to the metals, the oxidation potential dramatically decreases because of the high polarity of Re—C≡C—Re bonding. For example, the first oxidation process of *t*-butylacetylene, a representative aliphatic acetylene, cannot be observed to +2.0 V (vs Ag) in CH_3CN, whereas the corresponding oxidation process of 1 occurs at a much less positive potential as indicated above.

A striking feature of the electronic absorption spectrum of 1 is the presence of several resolved electronic transitions (Figure 5). The lowest energy absorption at 319 nm (31 350 cm^{-1}) is of moderate intensity (ϵ = 12 000 M^{-1} cm^{-1}) followed by two more intense absorptions at 242 nm (41 320 cm^{-1}, ϵ = 50 000 M^{-1} cm^{-1}) and 223 nm (44 840 cm^{-1}, ϵ = 68 000 M^{-1} cm^{-1}). These undoubtedly correspond to electric dipole allowed transitions. The lowest energy excitations obtained by SCF-Xα-DV transition-state calculations (Table V) show a similar grouping into three energies, although the optical gap appears to be underestimated by ~7000 cm^{-1}. Given the minimum basis set used, as well as the absence of relativistic corrections and configuration interaction in the Xα calculations, errors of 1 eV (8000 cm^{-1}) for excited states are to be expected. The 13 e_u → 13 e_g and 13 e_u → 14 e_g transitions (C≡C π → CO π^*) are tentatively assigned to the first broad absorption, the 17 a_{1g} → 17 a_{2u} and 17 a_{1g} → 14 e_u transitions are assigned to the second absorption, and 12 e_g → 17 a_{2u}, followed by excitations from 12 e_u, 15 a_{2u}, 3 b_{1u}, and 3 b_{2g}, to the third electronic absorption band. The weaker intensity of the first transition can be attributed to the small amount of d-orbital character in the 13 e_u orbital. All the lowest unoccupied orbitals are of CO π^* character and the most intense transitions in nonmetal–metal bonded binary carbonyls arise from electronic transitions with dπ → COπ^* character.

The electronic absorption spectrum of 1 can be compared with that of $Re_2(CO)_{10}$, whose lowest dipole allowed electronic transition $\sigma \rightarrow \sigma^*$ occurs at 32 800 cm^{-1} (24 000 M^{-1} cm^{-1}) followed by $\sigma \rightarrow$ CO π^* at 36 000 cm^{-1} (18 000 M^{-1} cm^{-1}) and d$\pi \rightarrow$ CO π^* 38 100 cm^{-1} (12 500 M^{-1} cm^{-1}).[16] Thus, the C≡C $\pi \rightarrow$ CO π^* transition in 1 (31 350 cm^{-1}) occurs at lower energy than the $\sigma \rightarrow$ CO π^* absorption in $Re_2(CO)_{10}$. This is consistent with our previous conclusions about the relative ease of oxidation of the C≡C π electrons in 1 relative to the metal–metal σ-bonding electrons in $Re_2(CO)_{10}$.

Experimental Section

Electrochemical Measurements. Acetonitrile and dichloromethane were distilled from CaH_2 under nitrogen. Tetrahydrofuran was distilled from potassium under nitrogen and then vacuum transferred for storage under nitrogen in a Schlenk flask. Tetra-*n*-butylammonium perchlorate (Southwestern Analytical Chemicals) was recrystallized for use as the supporting electrolyte by using ethyl acetate (HPLC grade) and isooctane (Burdick and Jackson).

Cyclic voltammetry measurements were performed using a BAS-100 electrochemical analyzer and BAS Model PL-10 digital plotter. The electrochemical cell was a locally constructed three-compartment cell with fritted glass dividing the compartments. A silver wire reference electrode was used. The potential for the ferrocene/ferrocenium couple was 0.38 V (CH_3CN) and 0.19 V (CH_2Cl_2) vs the silver wire reference. The platinum disk working electrode and the platinum wire auxiliary electrode were purchased from IBM Instruments. The working and auxiliary electrodes were cleaned with aqua regia before use. The working electrode and the reference electrode were polished with alumina.

Typically, a background cyclic voltammogram was recorded of a 0.1 M solution of the tetra-*n*-butylammonium perchlorate (TBAP) supporting electrolyte. Then, a solution 1×10^{-3} M in 1 and 0.1 M in TBAP was put into the cell compartment with the working electrode, and cyclic voltammograms were recorded at several scan rates after IR compensation.

UV–Visible Spectroscopy. Tetrahydrofuran was distilled from potassium under nitrogen. The electronic absorption spectrum of a 9.3×10^{-6} M solution of 1 in THF was recorded from 500 to 200 nm.

Theoretical Calculations. Electronic structure calculations were performed with the use of a DEC Micro VAX II computer and employed the self-consistent field discrete variational α (SCF-DV-Xα) method.[17] Numerical atomic orbitals from exact Hartree–Fock–Slater calculations were used with the α values of Schwartz.[18] For Re the orbitals through 6p were used as basis orbitals and the 1s–4d functions were treated as a frozen core orthogonalized against valence orbitals. A 1s, 2s, 2p basis was used for carbon and oxygen. The molecular Coulomb potential was calculated by a least-squares fit[19] of the model electron density to the numerical density. Seven radial degrees of freedom were allowed in the expansion function, in addition to the radial atomic densities. The experimental structure of 1 was idealized to D_{4h} symmetry for the calculations. The coordinate system assumes *z* coincident with the 4-fold axis and the CO groups to lie in the *xz* or *yz* planes.

X-ray Crystal Structure Determination. A crystal (0.15 mm × 0.15 mm × 0.05 mm) was fixed in vacuo in a Mark tube with an adhesive. Crystal data: $C_{12}O_{10}Re_2$, M = 676.5 g·mol^{-1}, space group $P\bar{1}$, a = 652.8 (2), b = 651.6 (2), c = 987.2 (2) pm, α = 90.40 (2), β = 96.77 (3), γ = 98.62 (3)°, V = 0.4122 (2) nm^3, Z = 1, μ(Mo Kα) = 149.2 cm^{-1}. Data collection with a Nicolet-R3 diffractometer at 20 °C, ω-scan, 4° < 2θ < 50°, scan speed 4–30°/min (minimum at $I < 400$, maximum at $I > 3000$ counts/s), measured reflections 3651, equivalent reflection averaged 1882 (R_{merge} = 0.0223), observed reflections 1749 [$I > 2\sigma(I)$], data corrected empirically on the basis of 11 φ scans (φ = 0–360° every 10°) for χ values near 90°. Solution and refinement: SHELXTL

(16) Levenson, R. A.; Gray, H. B. *J. Am. Chem. Soc.* **1975**, *97*, 6042.
(17) Ellis, D. E.; Painter, G. S. *Phys. Rev. B: Solid State* **1970**, *2*, 2887.
(18) Schwartz, K. *Phys. Rev. B: Solid State* **1972**, *5*, 2466.
(19) Delley, B.; Ellis, D. E. *J. Chem. Phys.* **1982**, *76*, 1949.

program, Patterson and Fourier recycling, refined parameters 109, $R = 0.067$, $R_w = 0.063$ [$w = 1/\sigma^2(F) + 0.0007F^2$].

Acknowledgment is made to the Deutsche Forschungsgemeinschaft and Fonds der Chemischen Industrie for generous support. W.C.T. thanks the Air Force Office of Scientific Research (AFOSR-86-0027) for financial support.

Supplementary Material Available: A table of structure factors (Table S1) (10 pages). Ordering information is given on any current masthead page.

Formation of Iridalactones by CH_2–O Oxidative Addition of Propiolactone to Iridium(I)

Andrei A. Zlota, Felix Frolow, and David Milstein*

Department of Organic Chemistry, The Weizmann Institute of Science, Rehovot 76100, Israel

Received December 4, 1989

Propiolactone undergoes facile oxidative addition to low-valent electron-rich Ir(I) complexes. $(C_8H_{14})Ir(PMe_3)_3Cl$ (1) yields the structurally characterized iridalactone *mer*-$(CH_2CH_2CO_2)Ir(PMe_3)_3Cl$ (2) by cleavage of the CH_2–O bond. The reaction is first order in both the lactone and 1. A likely mechanism involves nucleophilic attack by a 16-electron iridium complex on the CH_2–O carbon atom. The structure of 2 has been determined crystallographically [space group $P2_1/c$; $a = 13.184$ (5) Å, $b = 13.852$ (2) Å, $c = 12.761$ (4) Å; $\beta = 111.20$ (5)°; $Z = 4$; $R = 0.033$ for 4882 reflections].

Introduction

As part of our interest in the reactivity of C–O bonds of small ring compounds with low-valent, electron-rich metal complexes[1] we have examined the possibility of C–O oxidative addition of lactones to Ir(I). Although metallalactones may be intermediates in various reactions catalyzed by transition-metal complexes involving generation or transformation of lactones, isolation of such complexes is not common and most examples involve group 10 metals.[2] Recently, a rhodalactone was isolated,[3] and its relevance to the transition-metal-catalyzed cyclization of alkynoic acids to alkylidene lactones probed.[4] Oxidative addition of allyl and phenyl esters was observed.[5]

To our knowledge, the only example of oxidative addition of a lactone to a transition metal [Pt(II)] resulting in an isolable metallalactone was reported recently[2a] while this work was in progress.

Since the complex $(C_8H_{14})Ir(PMe_3)_3Cl$ (1, C_8H_{14} = cyclooctene) is known to undergo facile C–O oxidative addition of epoxides,[1a] we have examined its reactivity, as well as the reactivity of other electron-rich Ir(I) complexes, with β-propiolactone. Indeed, five-membered iridalactones can be directly formed by oxidative addition of the CH–O bond of β-lactones to Ir(I).

(1) (a) Milstein, D.; Calabrese, J. C. *J. Am. Chem. Soc.* **1982**, *104*, 3773. (b) Milstein, D. *J. Am. Chem. Soc.* **1982**, *104*, 5227. (c) Milstein, D. *Acc. Chem. Res.* **1984**, *17*, 221.

(2) (a) Aye, K. T.; Coipitts, D.; Ferguson, G.; Puddephatt, R. J. *Organometallics* **1988**, *7*, 1454; (b) Hoberg, H.; Peres, Y.; Krüger, C.; Tsay, Y.-H. *Angew. Chem., Int. Ed. Engl.* **1987**, *26*, 771. (c) Yamamoto, T.; Sano, K.; Yamamoto, A. *J. Am. Chem. Soc.* **1987**, *109*, 1092. (d) Hoberg, H.; Peres, Y.; Milchereit, A. *J. Organomet. Chem.* **1986**, *307*, C41. (e) Hoberg, H.; Schaefer, D.; Burkhart, G.; Krüger, C.; Romão, M. J. *Ibid.* **1984**, *266*, 203. (f) Sano, K.; Yamamoto, T.; Yamamoto, A. *Bull Chem. Soc. Jpn.* **1984**, *57*, 2741. (g) Yamamoto, T.; Tshizu, J.; Yamamoto, A. *Ibid.* **1982**, *55*, 623. (h) Yamamoto, T.; Yamamoto, A. *Chem. Lett.* **1984**, 941; **1983**, 115; **1982**, 695. (i) Yamamoto, T.; Tshizu, J.; Komiya, S.; Yamamoto, A. *J. Am. Chem. Soc.* **1980**, *102*, 7448.

(3) Marder, T. B.; Chan, D. M.-T.; Fultz, W. C.; Milstein, D. *J. Chem. Soc., Chem. Commun.* **1988**, 996.

(4) Chan, D. M.-T.; Marder, T. B.; Milstein, D.; Taylor, N. J. *J. Am. Chem. Soc.* **1987**, *109*, 6385.

(5) Yamamoto, A. *Organotransition Metal Chemistry-Fundamental Concepts and Applications*; Wiley: New York, 1986; pp 233–236 and references therein.

Table I. Experimental Crystallographic Data for 2

mol wt	574.04
space group	$P2_1/c$ (monoclinic)
temp, °C	−183
cell constants	
a, Å	13.184 (5)
b, Å	13.852 (2)
c, Å	12.761 (4)
β, deg	111.20 (5)
cell vol, Å^3	2173 (1)
formula	$C_{12}H_{31}O_2P_3ClIr\cdot{}^1/_2(C_7H_8)$
formula units/unit cell	4
D(calcd), g cm^{-3}	1.7548
μ(calcd), cm^{-1}	64
diffractometer/scan	Rigaku AFC5/ω–2θ
source	rotating anode Rigaku RU300
speed of measmt, deg min^{-1}	10
radiation, graphite monochr	Mo K$\bar{\alpha}$ (I = 0.7114 Å)
max cryst dimens, mm	0.15 × 0.15 × 0.15
no. of reflections	
measured	4882
duplicates	402
with $F_o > 3\theta(F_c)$	3860
θ_{max}, deg	54
R_{sym}	0.02
final R,R_w	0.033, 0.043

Results and Discussion

Addition of β-propiolactone to a toluene solution of 1 at −30 °C, followed by warming to room temperature, results in complete conversion to the iridalactone complex 2 (eq 1). This reaction proceeds even at −30 °C (requiring

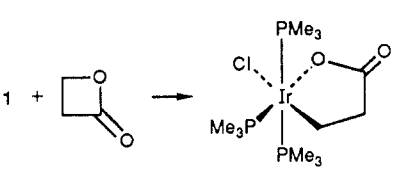

(1)

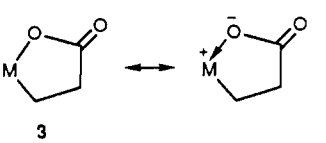

0276-7333/90/2309-1300$02.50/0